ACOUSTIC EMISSION DURING THE SCRATCH-TEST ON GALVANIZED STEEL

Rosa Piotrkowski
Escuela de Ciencia y Tecnología, Universidad Nacional de San Martín, Argentina.
Antolino Gallego
Dpto. Física Aplicada. E.U. Arquitectura Técnica, Universidad de Granada, Spain.
José Francisco Gil, Juan de Mata Vico, José Luis Piqueras, José Rodríguez
Dpto.Construcciones Arquitectónica, E. U. Arquitectura Técnica, Universidad de Granada, Spain.
José Evaristo Ruzzante
ENDE, Comisión Nacional de Energía Atómica, Buenos Aires, Argentina.

Keyworks: Coatings, galvanized steel, acoustic emission, scratch test, microfracture.

ABSTRACT

In this paper we evaluate coating-substrate adherence in galvanized steel with the Acoustic Emission (AE) technique applied during scratch tests (ST), analyzing in this way the elastic waves emitted during microfracture processes. Hot-dip galvanized samples were obtained, with different coating depths. Samples were obtained in Spain (Laboratory of Corrosion at the E.U. Technical Architecture) and ST with AE detection were performed at the Elastic Waves Laboratory, National Atomic Energy Commission, Argentina. The obtained AE were analyzed, in order to identify different fracture mechanisms by correlating them with microscopy observations. The final purpose was to establish adherence criteria that have to be connected with the manufacture process, thus leading to efficient quality control criteria.

1. Introduction

An efficient solution to problems related to the durability of reinforced concrete beams is obtained by using a coating of Zn (galvanized steel) to protect steel reinforcement from corrosion [1-3]. The use of this type of coating has nowadays been extended to different metallic applications. Although the coating-substrate adherence is high because during the coating forming process various Zn-Fe alloys are obtained, certain applications require a special quality control. Nevertheless, there exists a lack of total agreement on the type of adherence test to be used so as of established quality control criteria. In this paper we are proposing to evaluate this coating-substrate adherence with the Acoustic Emission (AE) technique applied to Scratch Tests (ST), analyzing in this way the elastic waves emitted during microfracture processes. Both ST and AE, previously applied to other metallic coatings [4], have not yet been used in the study of galvanized material. With this purpose, hot-dip galvanized were obtained, with different coating depths. Samples were obtained in Spain (Laboratory of Corrosion at the E.U. Technical Architecture) and ST with AE detection were performed at the Elastic Waves Laboratory, National Atomic Energy Commission, Argentina. The obtained AE was submitted to an analysis process, in order to identify the different fracture mechanisms, correlating them with optical microscopy, scanning electron microscopy observations and metallic chemical composition determination. The final purpose is to establish adherence criteria that have to be connected with the manufacture process, thus leading to efficient quality control criteria.

2. Experimental

2.1. Samples

Steel platelet samples 50 mm x 20 mm x 4 mm, were galvanized in EUROTEGA S.A., Spain, in a process that included successive stages. They were: degreasing bath at 80º C, elimination of iron oxide by immersion in water solution of 15% chloridric acid at 35º C, bath in water diluted ammonium chloride at 80º C, immersion in a Zn bath at 450°C and air cooling. Samples were then visually examined and the thickness of coatings was measured by the induced currents method.

Five batches of samples were obtained each of them consisting of 20 samples, according to the mean immersion time. Samples, hanging on vertical wires, were slowly introduced into the Zn bath. So, the immersion time was in fact different for samples corresponding to the same batch and for each sample itself. Because of this fact, the coating thickness of each sample was non-homogenous. Thickness assigned to each sample was the mean of three values measured at different points, with a dispersion of 20%. Moreover mean values were evaluated for each batch. According to this results samples were roughly classified according to coating thickness as High (H), $(200-220)\mu m$, Medium (M), $(140-150)\mu m$ and Low (L), $\cong 100\mu m$. Five samples of each class were selected for the present investigation. They were designated as L_i , M_i , H_i (i=1…5). Four of each class were assigned to scratching and AE tests and the fifth of each class to the assessment of the coating microstructure.

2.2. Coating Characteristics

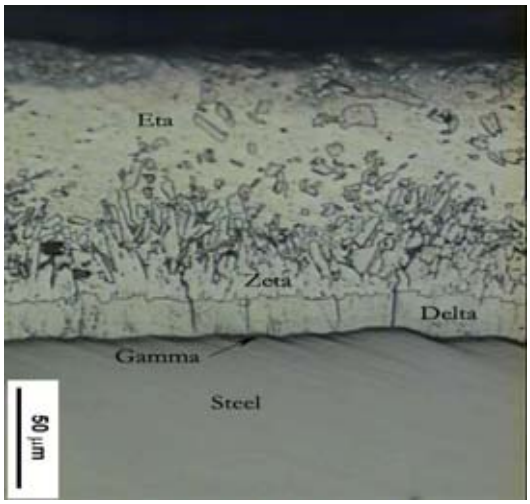

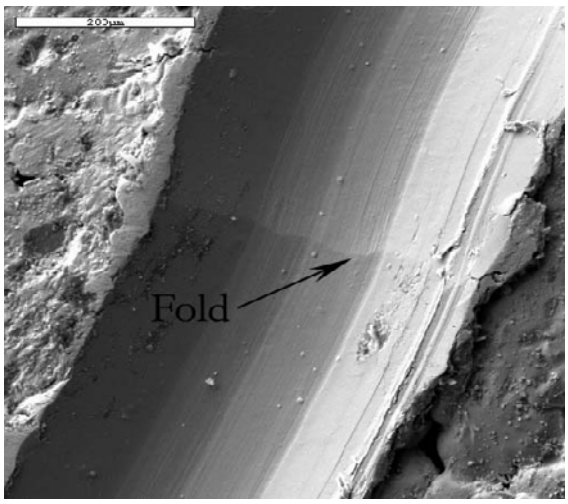

Figure 1 (Left): Transversal optical micrography of sample H_5. Zn-Fe coating phases.
Figure 2 (Right): Scanning electron microscope image of a fold (Scratch 1 of sample H_1).

Samples L_5, M_5 and H_5 were transversally cut and prepared for metallographic studies. Coatings were examined by optical microscopy, scanning electron microscopy and metallic composition was analyzed by EDX. Coatings were non-homogeneous and the matrix-coating interface boundary and the exterior surface were not plane at all. The different and well-known Zn-Fe phases were observed from steel to zinc (see Figure 1): gamma (a very thin and uniform layer along the coating), delta (very well defined), zetha (with small grains) and etha (almost pure Zn). Zetha and delta phases were in general intermingled, and their thickness showed a great variability along the coating. Moreover, in some points the zetha phase reached the exterior surface. These results were obtained by optical and EDX composition studies across coatings.

2.3. Scratch tests

Scratch tests were performed under controlled conditions with a device that consisted of a loaded probe with a diamond indenter moving linearly along the sample with a constant speed and linearly increasing force (0-150 N) during 180 s. The steadily increasing contact load causes tensile stress behind the indenter tip (trailing edge) and compressive stress ahead of the cutting tip (leading edge). The detection system used was MISTRAS 2001 from Physical Acoustics Corporation (PAC). The piezoelectric sensor was located with a coupling wax on the topside of samples. Then signals passed through preamplifiers (60 dB) and were measured by the AEDSP-32/16B card that has two channels for signal processing and wave shape determination. Threshold was set at 25dB, and signals were digitized at 4MHz/8bits for future work. In the present paper, the analyzed hit parameters were energy, cumulative energy through test, and cumulative number of hits through test. For the data analysis the software "Visual AE", of Vallen System, was used. ST with AE were performed on samples L_i , M_i , H_i (i=1…4). Three scratches were performed on each sample, with a length of approximately 1.1 cm. Optical microscopy images with high magnification were obtained along scratches on samples H_1, M_1 and L_1, and they were composed as a unique image with adequate software. Scratches were also observed with scanning electron microscope and the metallic chemical composition along each scratch (taking account that the penetration depth increases with the indenter advance) was assessed with EDX. Table 1 shows a layout of the experimental work.

		Low thickness					**Medium thickness**					**High thickness**				
		L_1	**L_2**	**L_3**	**L_4**	**L_5**	**M_1**	**M_2**	**M_3**	**M_4**	**M_5**	**H_1**	**H_2**	**H_3**	**H_4**	**H_5**
Scanning Electrom Microscope with EDX	**Chemical analysis along scratch**	X					X					X				
	Chemical analysis across coating					X					X					X
Optical microscope	**Composed optical microscope image of a scratch**	X					X					X				
	Low magnification photographs of scratch	X	X	X	X		X	X	X	X		X	X	X	X	
	Transversal optical micrograph of coating					X					X					X
AE equipment	**Scratch-Test with EA**	X	X	X	X		X	X	X	X		X	X	X	X	

Table 1: Tests and analysis performed on samples

3. Results

Optical microscope images of scratches show that the line widens as penetration increases. Moreover, scratches are not straight lines; some deviation occurs, which is especially

noticeable in H samples. This is due to the coating heterogeneity: the diamond tip had to go around the heterogeneous obstacles that could be the zetha phase grains, in the points where they reached the surface. For shortness reasons, we do not present here the optical microscope composed image of scratches. A certain number of little marks appeared at the beginning of scratches, corresponding to plastic deformation of the coating. The relevant feature in all images (for all scratches and samples) was the presence of some apparent transversal cracks that revealed to be folds (material doubled over) when observed with the scanning electron microscope. This has the important meaning that the failure was interfacial. As example, in Figure 2 we can see a scanning electron microscope image of a fold appearing in scratch 1 of sample H_1. Noticeable folds appeared at certain positions, which are in Table 2. Chemical composition, determined with EDX, and scanning electron microcopy were performed along the central line of scratches for each class of samples. Figures 3 (a-c) show as an example the selected points for scratch 1 of sample H_1 and Table 3 show the obtained measured results for three stages of scratch (beginning, intermediate, and final).

	L_1	**M_1**	**H_1**
Scratch 1	54% and 70%	47% and 72%	51% and 73%
Scratch 2	54%, 65% and 81%	44%	43%
Scratch 3	70%	43% and 74%	50%

Table 2. Position of significant folds on scratches, measured in % of total scratch length (relative position)

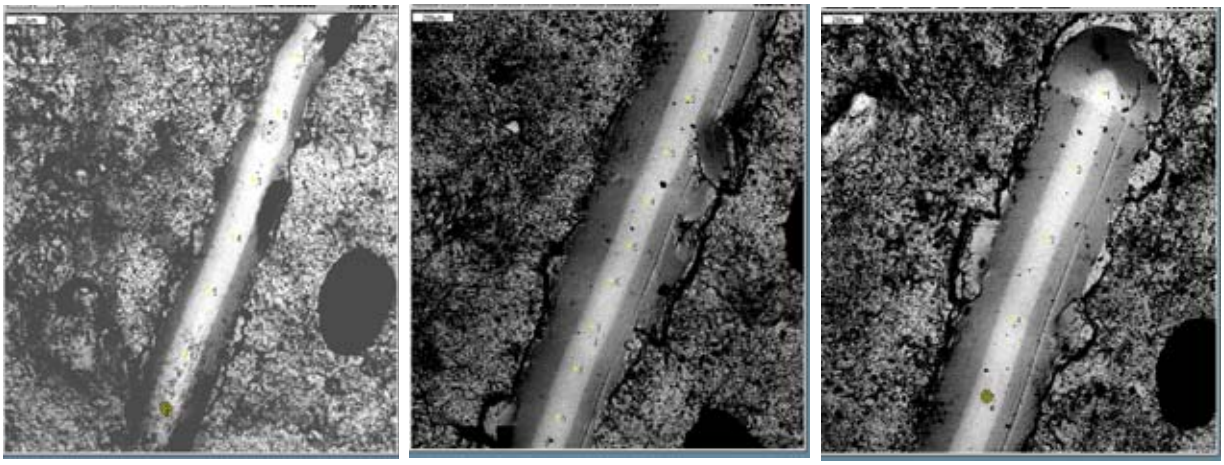

Figure 3a (Left): Scanning electron microscope image of scratch 1-sample H_1 (Beginning of scratch)
Figure 3b (Middle): Scanning electron microscope image of scratch 1-sample H_1 (Intermediate stage of scratch)
Figure 3c (Right): Scanning electron microscope image of scratch 1-sample H_1 (End of scratch)

	Beginning of scratch (Fig. 3a)		**Middle of scratch (Fig. 3b)**		**End of scratch (Fig. 3c)**	
Position	**Fe (%)**	**Zn (%)**	**Fe (%)**	**Zn (%)**	**Fe (%)**	**Zn (%)**
1	0,96	99,04	0,37	99,63	0,37	99,63
2	0,31	99,69	1,11	98,89	0,31	99,69
3	0,32	99,68	0,87	99,13	0,39	99,61
4	0,38	99,62	0,51	99,49	0,35	99,65
5	0,23	99,77	0,30	99,70	1,51	98,49
6	0,21	99,79	0,54	99,46		
7	0,26	99,74	0,38	99,62		
8			0,42	99,58		
9			0,34	99,66		

Table 3. Chemical composition at points shown in Figures 3 (a-c)

From these observations, we can deduce that in the first stages of scratching, the Fe % is low enough to infer that only the etha phase was reached. From an intermediate stage on, measurements suggest that the zetha phase could have been reached. This behavior holds till the final stage, so the indenter could have not touched the matrix, not even the delta and gamma phases. The non-uniformity of measured values accompanies the non-uniformity of etha and zetha phase distribution. If this is correct, the coating did not fail due to the matrix/coating interface detachment.

When AE parameters were analyzed, we found a strong correlation between AE and microscopic results. Figures 4 (a-c) show respectively the parameters energy, cumulative energy and cumulative number of hits for the scratch 1 of sample (H_1). The remarkable steps in cumulative parameters and peaks in energy, in graphs where the independent variable is the % of total scratch length, are very close to the position of folds in micrographs (showed in Table 2), and would correspond to gamma/zetha and zetha/etha interface positions. Figures 5 (a-c) and 6 (a-c) show similar results in scratch tests performed respectively on samples M_1 (scratch 3) and L_1 (scratch 2). It was observed that AE activity increased when the coating thickness decreased. Moreover the steps in cumulative energy, which corresponded to development of significant folds (see Table 2), showed up at lower % positions along scratch, that is to say at lower depths inside coating, when thickness was lower. Thus, coating performance improved when going from lower to higher thickness in the studied range. Results of the present paper constitute a step forward to recommend the use of AE parameters as indicators of coating failure, in on line measurements, instead of the a posteriori microscopic determinations. Future work will be related with the evaluation and comparison of hot-dip galvanized and electrolytic galvanized samples, with different coating thickness and different corrosion degrees.

4. Conclusions

Acoustic emission proved to be a good technique to assess coating/matrix adherence of galvanized steel as it did in previously studied coatings on metallic samples. The coating breakdown could have occurred by the adherence failure between etha/zetha and zetha/delta phases, but the matrix would have never been touched by the indenter in the range of forces applied in the present work (0-150 N). Coating performance improved with thickness in the range ($(100 - 200)\mu m$).

5. Bibliography

[1] G. Reumont, J.B. Vogt, A. Iost, J. Foct, “The effects of an Fe-Zn intermetallic-containing coating on the stress corrosion cracking behavior of a hot-dip galvanized steel”, Surface and Coatings Technology, nº 139, p.p. 265-271, 2001.
[2] A. Bautista, J.A. González, “Analysis of the protective efficiency of galvanizing against corrosion of reinforcement embedded in chloride contaminated concrete”, Cement an Concrete Research, Vol. 26, Nº2, p.p. 215-224, 1996
[3] K.W.J Treadway, B.L. Brown, R.N. Cox, “Durability of galvaniced steel in concrete”, Corrosion of reinforcing steel in concrete, ASTM STP 713, American Society of Testing and Materials, p.p 102-131, 1980.
[4] R. Piotrkowski, A. Gallego, J.E. Ruzzante and M.T. García-Hernández “Adherence of nitride coatings analyzed by acoustic emission signals coming from Scratch tests”, The eJournal of Nondestructive Testing & Ultrasonics, ISSN: 1435-4934. 2002.

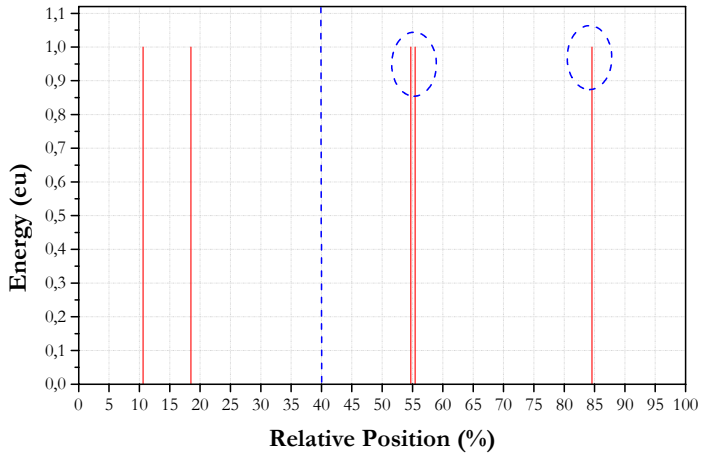

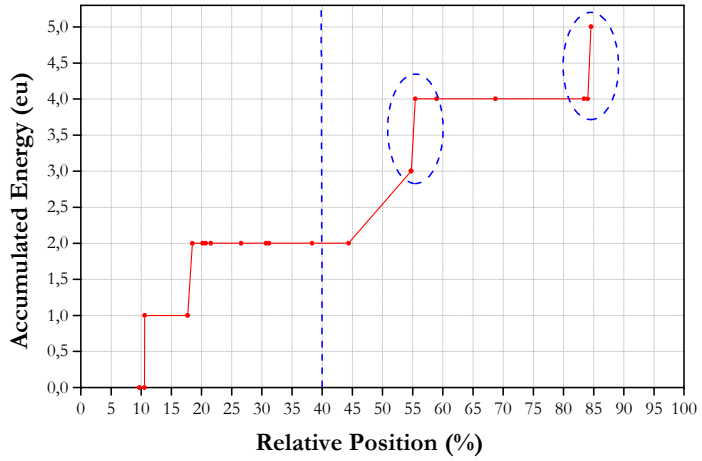

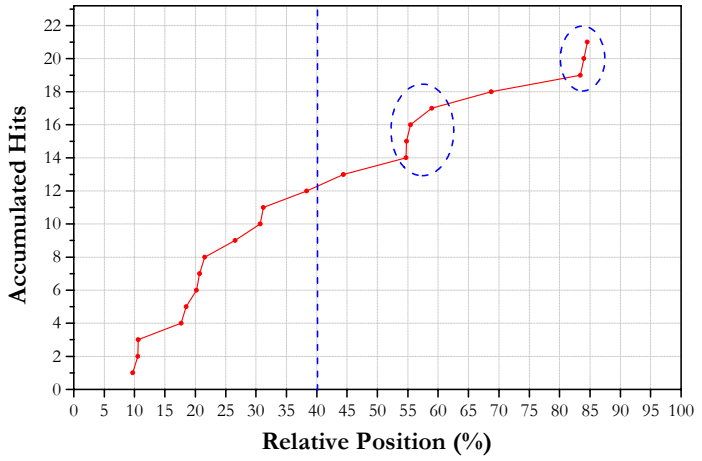

Figure 4 a (Up): Acoustic energy against relative position in %. Sample H_1. Scratch 1.
Figure 4 b (Middle): Accumulated acoustic against relative position in %. Sample H_1. Scratch 1.
Figure 4 c (Down): Accumulated number of hits against relative position in %. Sample H_1. Scratch 1.

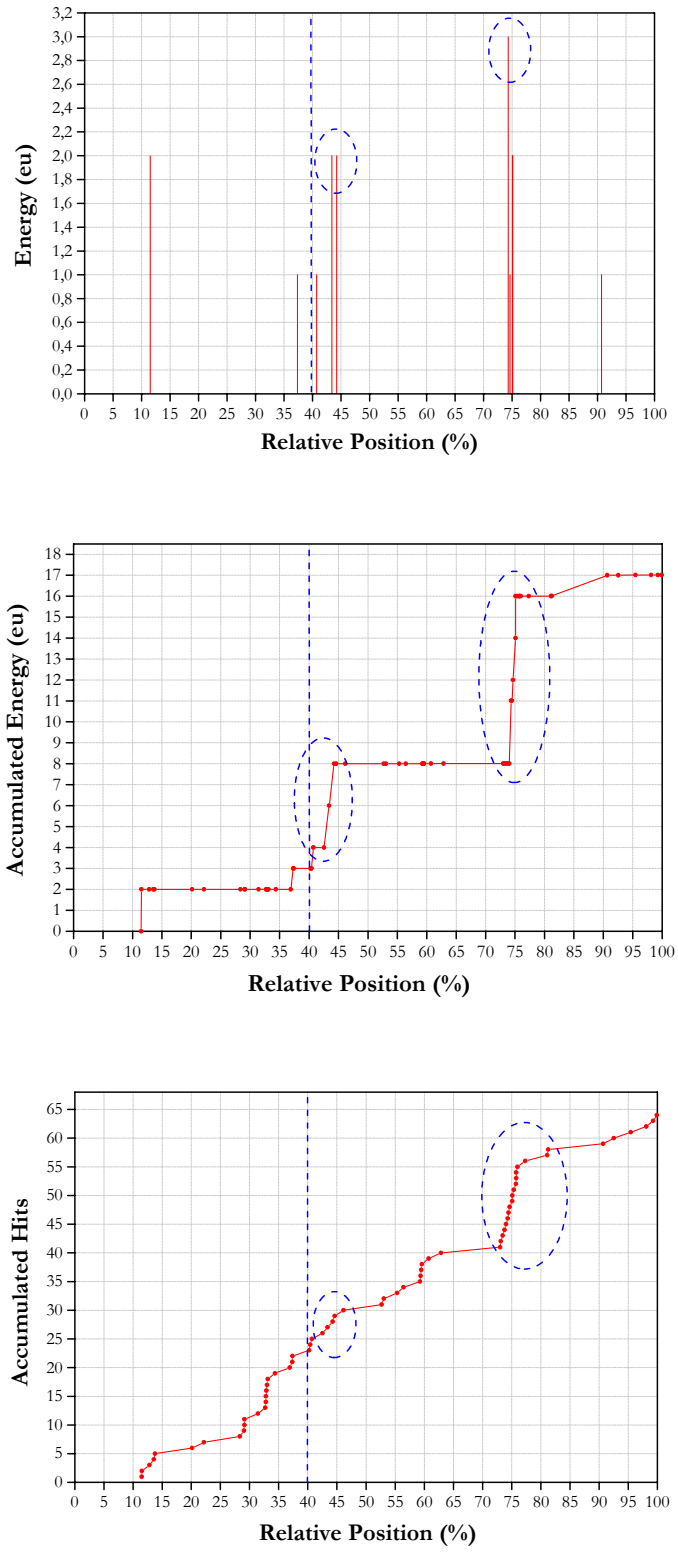

Figure 5 a (Up): Acoustic energy against relative position in %. Sample M_1. Scratch 3.
Figure 5 b (Middle): Accumulated acoustic against relative position in %. Sample M_1. Scratch 3.
Figure 5 b (Down): Accumulated number of hits against relative position in %. Sample M_1. Scratch 3.

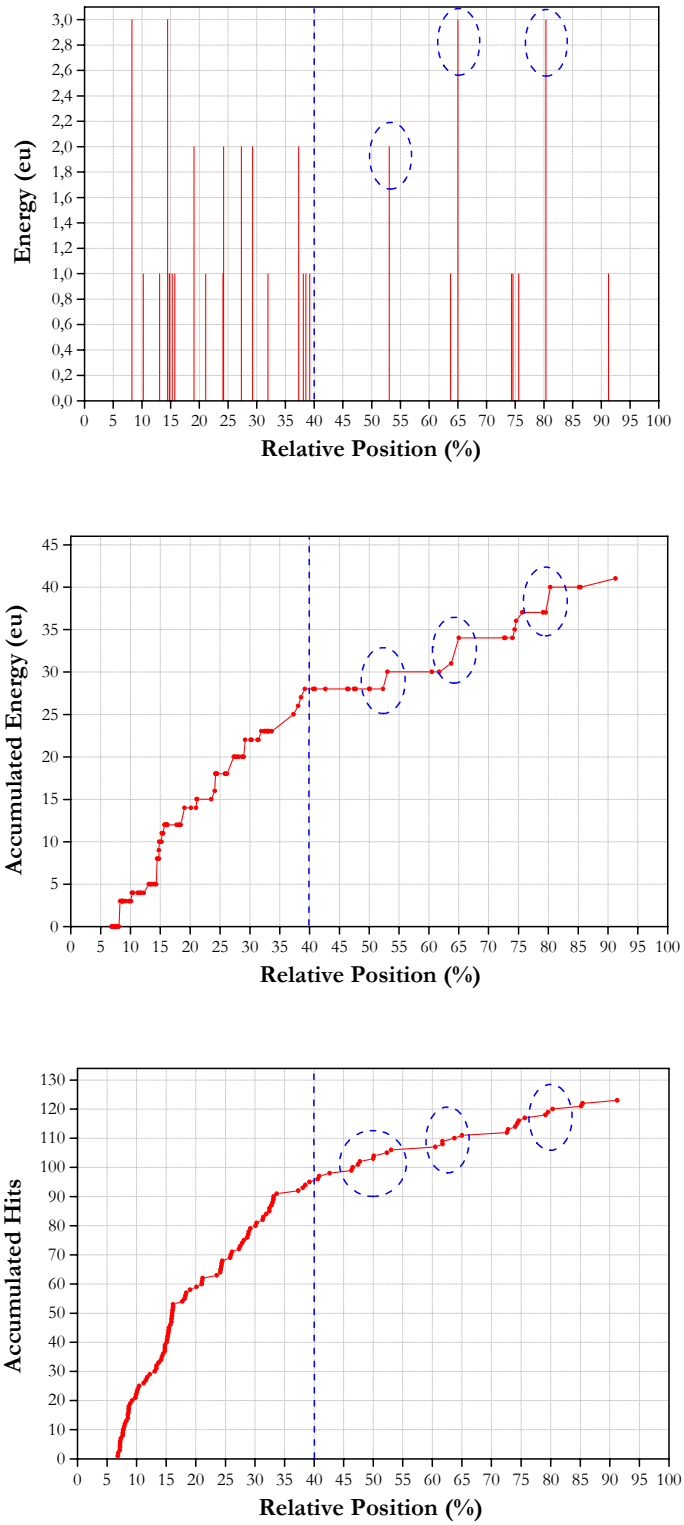

Figure 6 a (Up): Acoustic energy against relative position in %. Sample L_1. Scratch 2.
Figure 6 b (Middle): Accumulated acoustic against relative position in %. Sample L_1. Scratch 2.
Figure 6 c (Down): Accumulated number of hits against relative position in %. Sample L_1. Scratch 2.